Steve Kershaw · Yue Li · Sylvie Crasquin-Soleau · Qinglai Feng · Xinan Mu ·

Pierre-Yves Collin · Alan Reynolds · Li Guo

Earliest Triassic microbialites in the South China Block and other areas;

controls on their growth and distribution

S. Kershaw

Department of Geography and Earth Sciences, Brunel University, Uxbridge,

Middlesex UB8 3PH, UK

email: stephen.kershaw@brunel.ac.uk

Tel: +44-1985-266543

Fax: +44-1985-269736

Y. Li

Nanjing Institute of Geology and Palaeontology, 39, East Beijing Road, Nanjing

210008, China

S.Crasquin-Soleau and Pierre-Yves Collin

CNRS, UMR 5143 "Paléobiodiversité et paléoenvironnements", Université Pierre

et Marie Curie, T46-56, E.5, case 104, 75252 Paris cedex 05, France.

Q. Feng

Geosciences University, Wuhan 430074, Hubei Province, R.P. China

A. Reynolds

Experimental Techniques Centre, Brunel University, Uxbridge, Middlesex UB8

3PH, UK

L. Guo

CASP, Department of Earth Sciences, University of Cambridge, West Building,

181a Huntington Rd, Cambridge CB3 0DH, UK

Abstract Earliest Triassic microbialites (ETMs) and inorganic carbonate crystal

fans formed after the end-Permian mass extinction (c.251.4 Ma) within the basal

Triassic *Hindeodus parvus* conodont zone. ETMs are distinguished from rarer,

and more regional, subsequent Triassic microbialites. Large differences in ETMs

between northern and southern areas of the South China Block suggest

geographic provinces, and ETMs are most abundant throughout equatorial

Tethys Ocean with further geographic variation. ETMs occur in shallow marine

shelves in a superanoxic stratified ocean and form the only widespread

Phanerozoic microbialites with structures similar to those of the Cambro-

Ordovician, and briefly after the latest Ordovician, Late Silurian and Late

Devonian extinctions. ETMs disappeared long before the mid-Triassic biotic

recovery, but it is not clear why, if they are disaster taxa. In general, ETM

occurrence suggests that microbially-mediated calcification occurred where

upwelled carbonate-rich anoxic waters mixed with warm surface waters, forming

regional dysoxia, so that extreme carbonate supersaturation and dysoxic

conditions were both required for their growth. Long-term oceanic and

atmospheric changes may have contributed to a trigger for ETM formation. In

equatorial western Pangea the earliest microbialites are *late* Early Triassic, but

are predicted to occur in the earliest Triassic if suitable deposits are found.

Keywords microbialite . dendrolite . thrombolite . Permian-Triassic boundary .

anoxia . mass extinction

Introduction

Microbialites have been described from a range of sites in basal Triassic marine

sedimentary rocks in the immediate aftermath of the end-Permian mass

extinction (e.g. Erwin 2006; Wignall and Twitchett 2002) in the *Hindeodus parvus*

conodont zone. As microbially-mediated calcareous structures (Riding 2000),

these microbialites are readily distinguished from purely inorganic precipitates,

such as crystal fans, that also occur in Early Triassic limestones. The

microbialites are so widespread and distinctive that they warrant a collective

name, and are here termed Earliest Triassic Microbialites (ETMs). ETMs occur

either directly on, or a short distance above, the Permian-Triassic boundary

(PTB) "event horizon", the sharp boundary that marks rapid facies change in the

extinction. The event horizon lies below the biostratigraphic PTB (Krull et al.

2004), defined by the first appearance of the conodont *Hindeodus parvus* at

c.251.4 Ma (Erwin 2006). ETMs formed and disappeared well before the mid-

Triassic biotic recovery. Other microbialites later in the Early Triassic have been

identified in three intervals (Baud et al. 2006), but they occur in only a few places;

they are not included as ETMs in this study. Although ETMs have a wide

geographic distribution (Flügel 2002), they occur mostly within Tethys Ocean

(Fig. 1); details of literature records of their distribution are given later in this

paper.

Although problems of continental reconstruction mean that different

authors place continents in different locations, of great significance are the

profound differences between microbialites of the northern and southern margins

of the South China Block (SCB), because these lie within one continent, thus

proven to have been close together palaeogeographically. Significant differences

in microbialite structure are also reported from a range of sites globally; these

include stromatolites, thrombolites of different forms, calcimicrobes and various

clotted fabrics. At local scales in the SCB, individual microbial deposits vary in

sites only a few km apart. This range of variation (within the SCB, and between

the SCB and other areas) demands assessment in relation to environmental

change associated with the mass extinction. Consequently, this paper has two

aims: 1) to develop the first comprehensive synthesis of the structure and

distribution of global ETMs, using a compilation of detailed work in the SCB by

the authors, and literature descriptions of the SCB and other areas; and 2) to

apply evidence of global microbialite distribution and history to assess controls

on their formation in relation to published theories on the cause of the end-

Permian mass extinction. The study used a combination of fieldwork

observations, c.100 polished blocks, c.100 thin sections, SEM (secondary

electrons, backscatter electrons, and microprobe), and literature comparison.

Firstly ETMs of the SCB are described and compared, then global variation in

ETM form and distribution is outlined, and discussed against

palaeoenvironmental models.

Earliest Triassic Microbialites (ETMs) of the South China Block (SCB)

The SCB was a small tectonic plate through Palaeozoic to Triassic time, and

combined with other small plates during the Jurassic to form the present

landmass of China and neighbouring countries; until then the SCB was relatively

isolated. During the Permo-Triassic, the SCB was located in equatorial latitudes

of eastern Tethys (Fig. 1A); the northern shelf of SCB was a broad carbonate

platform, occupied by widespread Permian shallow-water carbonates and reefs,

which are overlain sharply by Triassic sediments. A major feature of the southern

shelf was the large Nanpanjiang Basin that was open to western Panthalassa
(Fig. 1B).

ETMs of Northern SCB (Sichuan, Chongqing & Hubei)

Well-exposed deposits of late Permian to Earliest Triassic limestones occur in
folded rocks immediately east of the Sichuan Basin, including a distinctive 1.4-c.3
m-thick microbialite biostrome (see Kershaw et al. 1999, and Ezaki et al. 2003 for
locality details). Although 3 m of rock is geologically a minor deposit, the
microbialite is widespread in eastern Sichuan and Hubei provinces, and the
Chongqing area (Kershaw et al. 1999, 2002; Ezaki et al. 2003; Yang et al. 2006).
Kershaw et al. (1999) referred to the microbialite as a "crust" on top of latest
Permian reef complexes, but in detail the microbialite grew on coarse and fine-
grained Permian carbonate sediments that overlie the reefs. The base of the
microbialite in all sites has stylolitic contact with underlying Changhsing
Formation limestones (Fig. 4B), therefore the exact nature of the microbialite
base is undetermined (Kershaw et al. 1999; Ezaki et al. 2003). However, lack of
any karstification or soils, or freshwater fabrics in the top of Changhsing
Formation is at least circumstantial evidence that there was no significant break.
There is no pebble lag at the base of the microbialite, and possibly the contact
simply represents an abrupt facies change. Field observations at Dongwan,
Baizhuyuan and Tudiya (near Chongqing) show that layering in the microbialite is

a mixture of sedimentary layers and stylolites. In the field, many stylolites are indistinguishable from sedimentary breaks and the correct number of layers has not been determined.

Regarding microbialite terminology, in the northern SCB, Ezaki et al. (2003) applied the classification developed for Cambrian thrombolites by Armella (1994: Fig. 4). Although the structure does contain a clear thrombolitic element, much of the microbialite has a digitate form (Kershaw et al. 1999) not fully matching either Armella's (1994) thrombolite, nor dendrolite defined by Riding (2000), except rarely (Fig. 4E). Therefore the term "digitate dendrolite" is used in this paper where appropriate. Of great importance, however, in the material studied here, is that the microfabric of both the thrombolite and digitate dendrolite architecture is the same, and underlines the problem of interpreting why the architecture should vary in fabrics which were presumably constructed by the same organisms. The microbialite is dominated by digitate dendrolites, plus thrombolitic layers (Figs. 2-7), and largely comprises a lobate architecture, suggesting it was composed of lobate objects compiled into digitate and thrombolitic form; unfortunately the structure is extensively recrystallised (Figs. 3 and 6, see also illustrations in Kershaw et al. 1999, 2002 and Ezaki et al. 2003), and has not yet been described from unaltered material. Also present are coccoid structures of possible bacteria (Mu et al. 2001; Ezaki et al. 2003; Yang et al. 2006). Sharp contacts between coccoid structures and recrystallised microbialite led Kershaw (2004) to suggest that the coccoid objects occupied cavities in the microbialite. Therefore the microbialite may have been built by

more than one microbial taxon. Particulate sediment throughout the microbialite

is micrite. Interlayers of shell-rich carbonate wackestones, packstones and

grainstones contain varying concentrations and sizes of small shelly fossils,

predominantly microgastropods. The interlayers are rich in peloids (Fig. 6), but

peloids are rare in micrite between branches of microbialite. The tops of some

microbialite layers are eroded (Fig. 5A), accentuated at the top of the microbialite

(Fig. 7). SEM microprobe examination confirms pyrite framboids in the sediments

of the microbialite, rich in Fe and S. Abundant Al indicates some clay in the

carbonate, which presumably accounts for the clay concentrations in the

abundant stylolites that cross-cut these beds. Secondary electron examination

shows the sediment is a consistently fine-grained micrite with no obvious

recrystallisation, in strong contrast to the microbialite branches. Figures 2-7

summarise the variation of microbialite structure in northern SCB, based on two

sites in Sichuan.

The microbialite can be traced around the nose of the plunging

Gaodingshan anticline near Huaying city, Sichuan, as a bed-parallel deposit in all

sites, although Wang et al. (1994) presented logs that show varying microbialite

thickness across the area, and absence in some sections. Wang et al. (1994)

also figured stromatolites above the dendrolitic microbialite in some sites.

Stromatolites were found in thin sections from above the microbialite in the

nearby Chuenmuping reef (observations by Li Guo), which is no longer exposed

due to quarrying. Variations in the sequence of microbialite sediments along

strike (Wang et al. 1994) are shown by detailed examination of two sites:

Baizhuyuan shows interbedded layers of thrombolitic and digitate dendrolite, in contrast to Dongwan, 1.3 km along strike, which lacks the thrombolite layers (compare Figs. 2 and 7). The microbialites have features in common with lithified modern shallow marine microbialites (Dill et al.1986; Dravis 1983); both are often smoothly abraded, and encrusted by marine cement, interpreted to have been aragonite because of its acicular form (Fig. 6).

ETMs of southern SCB

ETMs have been described from the Nanpanjiang Basin (Fig. 1B). ETMs occur on isolated carbonate platforms within the Nanpanjiang Basin (Lehrmann 1999; Lehrmann et al. 2003; Krull et al. 2004) as well as the platform margin (Liu et al. 2006). The microbialite biostrome lies on an eroded substrate of late Permian shallow marine limestones (Fig. 8) across most of the GBG. The eroded substrate consists of at least two episodes of deposition and erosion prior to microbialite colonisation (Fig. 8B). Recent discovery of meteoric fabrics (Collin et al. work in progress) supports an interpretation of subaerial exposure. However, the overlying microbialite is clearly aqueous, consistent with sea-level rise in the earliest Triassic. A c.15 m-thick biostromal framestone of "*Renalcis"*-type calcimicrobe (Fig. 8; see Lehrmann 1999 for illustrations of microfabric) grew in shallow shelf environments of the GBG. The framework consists of connected arches and patches of microbial carbonate, generating cryptic cavities, but no

cryptic biota have been found in the cavities. The framework is not uniform; in the

upper portions of the ETM biostrome, and in overlying biohermal patches, some

framework exhibits a vertical fabric, developing a dendrolitic character. Several

layers of shelly grainstones interrupt the microbialite (see Lehrmann 1999).

ETMs of other areas

Below is an outline literature survey of the global occurrence of ETMs, for

comparison with those of the SCB, emphasising just the relevant features. Riding

(2000) noted the problems of recognition of an organic origin in many microbial

carbonates, particularly those structures that have no modern counterparts.

Therefore, in the following list, those ETMs that are suspected to be inorganic, or

not proven to be within the *parvus* zone, are indicated.

Western Panthalassa Ocean; *Japan:* clotted peloids and crypto-microbial

stromatolites occur in the lowermost 5.5 m of Triassic strata (Sano and

Nakashima 1997), in a tidal flat located on a seamount, prior to accretion to the

Japan arc*.*

Southern Tethys; *1) Iran:* in the Zagros Mountains, 1 m-high thrombolite

mounds are associated with shallow marine peloidal grainstones at Abadeh

(Heydari et al. 2000). Extensive planar stromatolites, 6 m thick, occur at

Aliguordarz (Wang et al. 2005) (see Fig. 9 for an example), in marginal marine

sediments lacking biostratigraphic control but have the widely-distributed basal

Triassic negative $\delta^{13}C$ excursion (see Erwin 2006, for discussion of the

excursion). *2) Turkey:* stromatolitic and clotted fabrics occur in marine shelf facies complex of microbialites 10-42 m thick (Baud et al. 2005); microbialites occur in fine sediment, but overlying and underlying deposits are grainstones. Some stromatolites were probably inorganic crystal fans (Wignall and Twitchett 2002). Palaeogeographic reconstruction indicates the Iranian and Turkish sites were in Neo-Tethys (Fig.1).

Northern Tethys; *Hungary:* planar stromatolites, 8 m thick, contain clotted microbes (of *Angusticellularia*) above a mudstone, 0.5 m thick, in a deep ramp setting (Hips and Haas 2006; Haas et al. 2006).

Central Tethys; *Armenia:* 2 m-thick domal stromatolites occur, of both microbial structures and inorganic carbonate cement (Wignall and Twitchett 2002; Baud et al. 2006).

High latitudes*; 1) Greenland:* minor stromatolites occur in earliest Triassic marine clastics (Escher and Watts 1976; Perch-Nielsen et al. 1972), but are not fully described. *2) Tibet:* Garzanti et al. (1998) described "pseudostromatolites" from basal Triassic pelagic muds in south Tibet, but their nature is unconfirmed. *3) Madagascar:* Wignall and Twitchett (2002:403) noted 2 m-high stromatolites in an embayment of Tethys (Fig. 1), but age relationships are not fully established.

Wignall and Twitchett (2002) demonstrated that the earliest Triassic facies were dominated by low oxygen levels (dysoxia) in surface oceans. ETMs mostly developed in low-oxygen waters, the implications of which are discussed later. However, not all locations of earliest Triassic dysoxic waters contain ETMs; they are absent in dysoxic shallow marine sequences in western Tethys (Italy), and on

the margin of Gondwana (southern margin of Neo-Tethys), including Kashmir

and Pakistan (Brookfield et al. 2003; Wignall and Hallam 1993; Wignall and

Twitchett 2002). In contrast, dysoxia is not universal in the earliest Triassic,

revealed by two sites with higher diversity biotas, lacking evidence of both

dysoxia/anoxia and microbialites: **a)** in Oman (Twitchett et al. 2004), where there

is also a rapid return to positive δ^I C_{CARB} values of 3.1 ppt, interpreted by Krystyn

et al. (2003) as fast recovery from extinction; and **b)** in part of southern SCB

where high ostracod diversity in the earliest Triassic indicates well-oxygenated

conditions (Crasquin-Soleau et al. 2006). Furthermore, evidence from

microgastropods from several locations, globally, suggests that recovery from

mass extinction varied regionally, and was recently proposed to have begun

earlier than is traditionally interpreted (Fraiser et al. 2005). More evidence comes

from trace-making organisms, which took longer to recover in low latitudes

(Twitchett 2004), which may relate to oxygenation.

Microbialites later in Early Triassic

Microbialites are also found in sediments above the *parvus* zone. These are listed here to clarify they that are not included as ETMs:

Eastern Tethys; *Southern SCB:* sporadic "*Renalcis"*-type 1-m bioherms are found up to c. 200 m above the event horizon (Lehrmann 1999).

Western Tethys; *Italy*: small stromatolites (0.25 m thick) occur in the Tesero Site (Wignall and Hallam 1992), in dysoxic settings (Wignall and Twitchett 2002).

Western Pangaea; *Utah and Nevada in the Great Basin:* widespread small microbialite mounds occur in the late Early Triassic Moenkopi Formation (Smithian and Spathian) (Pruss et al. 2006). The lowermost Triassic stages (Griesbachian and Dienerian) are apparently missing, discussed by Alvarez and O'Connor (2002) and Bissell (1973).

Discussion

Global and regional processes potentially related to ETMs

To place ETMs in a geological perspective, they formed for a short time after the mass extinction, during rising sea level after the latest Permian lowstand (Erwin 2006). ETMs were widespread (Pruss et al. 2006; Baud et al. 2006), largely equatorial (Flügel 2002:400; Weidlich et al. 2003), and most abundant in the Cimmerian continents (Fig. 1) between NeoTethys and PaleoTethys (Wignall and Twitchett 2002). Similar microbialites occur abundantly in Cambrian and

13

Ordovician normal marine facies (Armella 1994; Kennard 1994); after then (apart

from the PTB, and other brief intervals discussed later) they declined, probably

due to increased grazing pressure concomitant with the mid-Ordovician biotic

radiation (see Sheehan and Harris 2004 for a review). So, in principal, the

organisms that created ETMs could have grown irrespective of mass extinction;

indeed some ETMs listed earlier in this paper occur in restricted settings and

could have developed even in the absence of mass extinction. However, the

widespread coincidence of ETMs for a short period indicates that they were biotic

responses to unusual ocean conditions (Kershaw et al. 1999; Lehrmann 1999;

Lehrmann et al. 2003; Ezaki et al. 2003; Baud et al. 2005), particularly those that

grew in open shelf environments. The potential controls on ETMs are considered

in the following list; some of the information is derived directly from geological

evidence, and some is from theoretical considerations and modelling. The

purpose is to assess the extent to which the processes, proposed to have

operated in association with the end-Permian mass extinction, could account for

ETMs.

Surface-ocean oxygen levels: Crasquin-Soleau and Kershaw (2005) used

ostracod data to suggest ETMs grew in oxygen concentrations of approximately

half that of modern seawater, consistent with a superanoxic ocean (Isozaki 1997;

Wignall and Twitchett 2002). Grice et al. (2005a) identified biomarkers in

Australia (southern Tethys), not in microbialites, that indicate anoxic

photosynthesis at the boundary, into the basal Triassic; it is possible that ETMs

contained a component that functioned by anaerobic productivity. Furthermore, Grice et al. (2005b) interpreted another biomarker as relating to acritarchs that indicate a unique ocean ecosystem in the Early Triassic. Nevertheless, although there is robust geological evidence for reduced oxygen levels in association with ETMs, low oxygen is unlikely to be the *only* control on ETMs because that is not consistent with the geological record of microbialites in normal seawater mentioned above.

Ocean carbonate supersaturation and storage: Microbial communities in general were probably facilitated by secular changes in ocean carbonate supersaturation (Riding 2005; Riding and Liang 2005), which may have created both organic (microbially-mediated) and inorganic (crystal fan) carbonate during the Permian and Triassic. However, if supersaturation was important in the formation of ETMs, then their patchy distribution and early termination within the *parvus* zone require consideration of ocean circulation. The superanoxic stratified ocean was sustained for a long period, and estimates vary between 8 millon years, with the first 1-3 million years being the most severe (Grice et al. 2005a), up to 20 million years (Isozaki 1997; Kidder and Worsley 2004). Although Winguth and Maier-Reimer (2005) suggested that the deep ocean circulation of those times was active, this goes against the established views on warm halothermal seas. Late Permian warm surface waters and a slow-circulating halothermal ocean are more likely (Beauchamp and Baud 2002), and should have led to deep-water storage of carbonate rich in ^{12}C, derived from a

combination of sulphate reduction (which creates bicarbonate, Kempe 1990),

ocean production and terrestrial runoff (that gets transferred to the deep ocean

by primary production). A coupled ocean-atmosphere model for the late Permian

(Kiehl and Shields 2005) predicts extreme stratification in Tethys Ocean, and a

slow deep ocean circulation might therefore lead to entrapment of stored

carbonate in Tethys. Also, Tethys is surrounded on three sides by land that may

be presumed to have delivered eroded terrestrial carbon to the sea during the

Permian, in a warm climate when sea level was falling. That carbon was

presumably already biased towards ^{12}C when it entered Tethys surface waters,

because some may have come from the Cimmerian continents; the SCB has

widespread Permian coal deposits (Wang and Jin 2000). The ocean store of

carbonate (probably principally as bicarbonate) could have been the principal

source material for ETMs.

Upwelling: Upwelling is the obvious mechanism to return anoxic deep water to

the surface, but there are several aspects that may relate to ETMs, discussed

here. *1)* Equatorial circulation in Tethys (Valentine and Moores 1973),

presumably led to upwelling driven by coriolis-driven Ekman transport

divergence. Figure 1 shows a proposed surface ocean circulation (Kidder and

Worsley 2004), with upwelling near the Cimmerian continents in Tethys. Ekman

transport should also have driven upwelling along the Tethyan margins, but

Kidder and Worsley (2004) interpreted sinking water in some areas (Fig. 1). *2)* In

a poorly-circulated ocean, patchy dysoxia of surface waters might result from

16

inefficient transfer of anoxic water to the surface. Conduits of upwelling of H_2S

from deep ocean to atmosphere (Kump 2005), may have been principally in low-

latitudes of Tethys, coinciding with ETM abundance, and providing a reason for

the records of uneven dysoxia. **3)** Kakuwa and Matsumoto (2006) used Cerium

anomaly data to support the view of upwelling of anoxic waters, and extended

the argument by presenting evidence of a rising anoxic water mass an estimated

600 ka before the PTB. Also Bottrell and Newton (2006) interpreted a short

episode of H_2S-rich ocean water at the PTB, based on sulphur isotopes. **4)** The

negative shift in $\delta^! C_{CARB}$ from +4 ppt (Late Permian) to –3 ppt (basal Triassic)

(e.g. Payne et al. 2004) may reflect ocean overturn following a long period of

ocean stagnation that caused a sustained high positive $\delta^! C_{CARB}$ value in shallow-

water limestones, although it has long been supposed that the excursion was

caused by productivity collapse. However, whatever caused the excursion (more

on this later), Payne et al. (2004) showed that it reversed early in the

Griesbachian, and approximately coincides with termination of ETMs in at least

two sites in the Great Bank of Guizhou. Of the later fluctuations of $\delta^! C_{CARB}$

(Payne et al. 2004), only one fully coincides with microbialite growth, in the

Spathian (see Pruss et al. 2006: Fig. 4). **5)** Rapid release of methane from

methane hydrates was postulated by Ryskin (2003), among other authors, to be

a cause of the mass extinction, might be focused in certain areas. Low-oxygen

bicarbonate-rich water carried to the surface by explosive release of methane

gas could lead to the recorded patchy distribution of microbialites. However, very

light carbon isotopes, -37 and –42 ppt in *organic* carbon, have been reported

17

from only one site (Sandler et al. 2006) in cores, and these are more problematic

to interpret than inorganic carbon isotopes. Furthermore, Payne et al. (2004)

noted that the repeated $\delta^{I} C_{CARB}$ excursions in the Early Triassic would need

recharge of the ocean sediment methane reservoir between excursions, and they

calculated there was not enough time to accumulate the amount of methane

required. *6)* Nutrients upwelled from the deep ocean might have stimulated

ETMs, but if acting alone should produce a *positive* ^{13}C shift (Saltzman 2005) not

the negative one observed. Modelling by Hotinski et al. (2001) concluded that a

large increase in the ocean nutrient content should be a component of the action

of upwelled anoxic waters. Also, upwelled nutrients should be dominated by

phosphate-limiting processes because anoxic waters cause denitrification (see

Kump et al. 2006; Saltzman 2005). Nevertheless, complex views were concisely

expressed by Berner and Ward (2006) and Kump et al. (2006), in relation to the

roles of H_2S, N and P nutrients and ocean circulation. As an illustration of the

problem, Kump et al. (2006) noted that even in the modern oceans, which are

vigorously circulating, there is stratification of nutrients driven by biotic

processes; how nutrients were distributed in the Late Permian halothermal

oceans, and how they might have influenced ETMs, is therefore open to

question.

Atmospheric changes: The effects of atmospheric CO_2 release by volcanic

sources (the Siberian Traps, which would also include SO_2) and terrestrial

weathering (Erwin 2006; Kaiho et al. 2006) could relate to ETMs. Sheldon (2006)

presented evidence of a sharp rise in terrestrial chemical weathering in Antarctica with a rapid shift to a basal Triassic greenhouse. Note, however, that the modelling and carbon isotope data, referred to earlier, indicate that the world was already in a greenhouse state, and sulphate aerosols from Siberian volcanics may have depressed atmospheric temperatures. Berner (2005) modelled a drop of atmospheric oxygen from c.30 % to c.13 % over a 20 my period in latest Permian and earliest Triassic that may relate to significant atmospheric perturbation; support for atmospheric deterioration comes from abnormal pollen in Russia and NW China (Foster and Afonin 2005), and from abrupt increase in soil erosion and export of terrestrial eroded products to the oceans (Sephton et al. 2005). Note also that evidence is poor for a major bolide impact at the PTB (Twitchett 2006). From the above information, the biggest problem for explaining the occurrence of ETMs in relation to atmospheric changes is whether those changes can have been rapid enough to account for the sharp lower and upper margins of ETMs. Presumably, large quantities of CO_2 (and possibly SO_2) dissolved directly into seawater from the atmosphere would inhibit carbonate precipitation, and so atmospheric controls would need to have entered the ocean via dissolved carbon in river waters, seemingly a much slower process than ocean upwelling.

A scenario of ETM formation

From the range of potential controls of ETMs outlined above, in general we interpret ETMs developed when and where the barrier between surface and deep ocean waters was overcome by upwelling of supersaturated anoxic waters, principally in Tethys. Although it is possible that mass extinction of skeletal biotas made carbonate available for ETMs directly in the Early Triassic surface ocean, the disappearance of ETMs long before skeletal recovery means another source of carbonate is required. The profound atmospheric changes (for which there is both modelling prediction and undisputable geological evidence referenced in this paper) may have contributed to ocean stratification instability, but the sharp changes in ocean facies and biota in the extinction interval are more easily explained by abrupt changes in ocean state. Thus the "bottom-up" approach of ocean upwelling is favoured over the "top-down" approach of atmospheric driving forces as the prime stimulus for ETM formation. However, the absence of ETMs in some dysoxic areas might be attributable to insufficient supersaturation of upwelled waters. This scenario is similar to that which produced inorganic carbonate crystal fans in the Early Triassic (Woods et al. 1999). The three episodes of microbialites later in the Early Triassic (Baud et al. 2006; two of which include crystal fans, Pruss et al. 2006) are regionally restricted and may indicate subsequent pulsing of upwelling in only those areas. Perhaps the initial pulse of upwelling in the earliest Triassic sufficiently depleted the deep water carbonate store to prevent further upwelling events from permitting widespread carbonate deposition.

Whatever the mechanism, if upwelled anoxic waters brought high concentrations of bicarbonate into the surface waters, then large quantities of nutrients would come up as well. Although the negative carbon isotope excursion is often viewed as creating productivity collapse, upwelled nutrients (especially phosphorus, see Kump et al. 2006 and Saltzman 2005) should have driven productivity and contributed to the development of ETMs, and should be reflected in a *positive* excursion (Saltzman 2005). If the ocean overturn carried up light carbon then the negative excursion observed might be due to the overwhelming effect of upwelled deep water (pushes isotopes towards negative) masking a drive towards positive values in microbial productivity. Note also that the Late Permian carbon isotope trend shows a consistent positive level of +3 to +4 ppt, which is actually the level of the peak of most positive excursions in the Palaeozoic; it could be argued that the negative shift of carbon isotopes at the PTB briefly returned the ocean towards more normal isotope levels (Brad Cramer, personal communication to SK), but overshot towards negative, because of the dominant content of upwelled light carbon. If upwelling was geographically limited, then dysoxic waters could have spread quickly across the global shallow ocean via circulatory gyres (Fig. 1).

Once the overturn had taken place, if stratified ocean conditions were re-established, then decline of supersaturation in the surface waters could be the cause of termination of abundant microbialite growth. It is unclear why ETMs are not preserved in the equatorial western Pangaea locations of Nevada and Utah, given that the model by Kiehl and Shields (2005) predicts upwelling there. The

problem may be bad preservation of earliest Triassic facies (Alvarez and

O'Connor 2002), so we predict that ETMs might be found in those locations in

future work.

Small-scale controls on Microbialites

On a small scale, many ETMs in the SCB are interbedded with carbonate

sediments rich in shelly faunas of well-preserved microgastropods and ostracods

as described earlier. Such facies show small-scale fluctuations in ETM formation

that might be due to localised shifts in surface-water conditions. For example, in

the northern SCB sites examined, peloids are rare between microbialite

branches, but rich in the interlayers. The gastropod-rich sediment interlayers may

represent short episodes of increased oxygenation which interrupted microbialite

growth, most likely associated with turbulence. It follows that the microbialite

layers may have grown in low-energy water (because of fine-grained sediment),

which suggests a decline in energy of ocean-surface circulation in the earliest

Triassic; more work is required to address this intriguing possibility.

Histories of individual ETMs show that there was further overprinting of

local changes onto the larger-scale controls. For example, Liu et al. (2006)

reported 3 shallowing-up cycles in ETMs of the southern SCB. By comparison,

some *northern* SCB ETMs have vertical changes that suggest cycles also existed

within those sequences, although they are not well defined. Figure 5A shows

that, within the microbialite, tops of microbialite layers are eroded. Figure 7

shows a minor episode of erosion of domes and deposition of shelly micrite

occurred near the top of the Dongwan sequence before the final microbial growth

(Figs. 5B and 5C); this differs from larger-scale erosion, such as that illustrated

by Goldhammer et al. (1993:Fig. 7F) in Ordovician sponge-algal bioherms in

west Texas. In contrast, the erosion is not recorded in the nearby Baizhuyuan

site, 1.3 km along strike from Dongwan (Fig. 2). We interpret the minor erosion at

Dongwan indicates that the effects of shallowing on the microbialites was limited,

possibly to local topographic highs, and did not proceed to intertidal facies.

Another local difference is shown by the presence of sheets of thrombolite

interlayered with digitate dendrolite at Baizhuyuan (Fig. 2), but not in Dongwan.

The digitate dendrolite form could have been an adaptation to higher

sedimentation rates in some places.

Regional microbialite diversity

Regional differences in microbial types and architectures suggest biotic

provinces of microbial forms; Turkey, Iran and South China Block have highly

contrasting assemblages of ETMs described earlier in this paper, in open marine

environments. Plate reconstructions vary, and the relative location of Turkey, Iran

and south China is not the same in all reconstructions. However the northern and

southern SCB are proven neighbours, and show major differences of microbial

communities and architectures (Kershaw et al. 1999; Ezaki et al. 2003; Lehrmann, 1999) (Fig. 2). In northern SCB, in an open shelf setting, ETMs form a single unit on the event horizon that does not reappear (Kershaw et al. 1999). In southern SCB, the Great Bank of Guizhou (GBG) has restricted marine facies and peritidal sequences where *"Renalcis"*-like framestones are repeated in cycles in the platform, in prolonged restricted conditions (Lehrmann et al. 2001).

Geographic isolation may have prevented intermixing of microbes, but two examples show how further research is needed to understand the community controls. **1)** ETMs in northern and southern SCB are only c.600 km apart, and in palaeogeographic reconstructions there is no proven land between them (Tong and Yin 2002; Wang and Jin 2000). Reasons for differences in microbial assemblages may relate to shallow-water circulation on the SCB. Note also that southern SCB faced Panthalassa Ocean, while northern SCB faced eastern Tethys (Fig. 1), which may have implications for the microbial communities. **2)** Within Tethys, Crasquin-Soleau and Kershaw (2005) demonstrated similarity between ostracod faunas in northern SCB and Turkey. The two areas were sufficiently close for dispersion of benthic species such as ostracods, yet the microbialites are different. The reasons for this inconsistency may relate to local environmental controls.

Were ETMs anachronistic disaster biotas?

Sepkoski et al. (1991:310) interpreted the earliest Triassic facies to have been anachronistic, meaning that the earliest Triassic presents a re-run of earlier Earth-surface environments; this concept has been adopted by many subsequent authors. Both the late Precambrian (Grotzinger and Knoll 1995) and Early Palaeozoic (Fang 2006) have been proposed as having similar environments to the earliest Triassic. However, if the semi-enclosed nature of Tethys is partly the reason for extreme stratification (Kiehl and Shields 2005), followed by overturn and release of long-term storage of bicarbonate, then those conditions are unique to the earliest Triassic. Therefore the application of the anachronism concept to ETMs is questionable.

Also problematic is whether the "disaster taxa" concept (Schubert and Bottjer 1992) is applicable to ETMs or not. On one hand, ETMs seem to have been limited to low oxygen conditions, which supports the disaster taxa idea. On the other hand, because the Early Triassic biotic crisis extended for c.4 Ma, thicker deposits of ETMs should be present; but ETMs are very thin deposits and there is no clear increase in Early Triassic calcimicrobes following the end-Permian extinction. If, however, the microbialites were also controlled by carbonate saturation (cf. Riding 2005; Riding and Liang 2005), then a direct link between abundance of microbialites and lack of higher life forms is weakened. Because of these inconsistencies, categorization of ETMs as disaster taxa is not straightforward, and debate will continue on the application of this concept.

To complete this discussion, PTB microbialites are the thickest, most extensive and most diverse of any microbialites formed after mass extinctions,

and brief comments on other extinctions provide a useful perspective. *1)* Short episodes of microbialites after the Late Ordovician in North America (Sheehan and Harris 2004) are actually largely in tidal flat settings according to those authors, and we wonder to what extent there is a direct link between the Late Ordovician extinction and proposed microbial resurgence. *2)* In the Late Silurian small-scale Lau extinction event, microbial and other fabrics are associated with the largest positive $\delta^{13}C$ excursion of the Phanerozoic (Calner 2005); if positive excursions relate to nutrient input that stimulated production (Saltzman 2005), microbial facies might have been promoted after extinction. If there was a comparable positive excursion in the earliest Triassic, it was swamped by negative-trending inputs, as discussed earlier. *3)* Finally, the Frasnian-Famennian (F/F) (Whalen et al. 2002) extinction in Canada is accompanied by thrombolites that grew in fully marine conditions, in parallel with ETMs; indeed Chen et al. (2002) predicted widespread anoxic conditions and associated cyanobacterial blooms following the F/F. In all these three cases, and the PTB, environmental changes promoted microbial growth, but explaining all of them by only anachronism and disaster forms is an oversimplification; evidence and argument presented in this paper support views that facies control and carbonate saturation are important components in the geological record of post-extinction microbialites.

Conclusions

This study draws the following conclusions about the earliest Triassic microbialites (ETMs):

1. The microbialites responded opportunistically to low concentrations of surface-water oxygen and high levels of carbonate supersaturation in the post-extinction superanoxic ocean that had developed through the Late Permian; these processes are exemplified by ETMs of south China. Low oxygen conditions maintained suppression of skeletal biotas and promoted anaerobic photosynthesis, while elevated carbonate supersaturation promoted microbially-mediated calcification.

2. The major microbialite deposits are in the Cimmerian continents of south China, Turkey and Iran; their low-latitude positions coincide with model predictions of positions of upwelling of anoxic bicarbonate-rich deep ocean water, principally in central Tethys Ocean.

3. The microbialites are much more diverse than has been fully appreciated in the literature. It seems, as far as microbia are concerned, that the earliest Triassic was a time of opportunity for microbial communities to develop regionally distinctive deposits.

4. A combination of atmospheric and oceanic processes may have built up carbonate storage in the Late Permian deep Tethys waters to a trigger point when overturn caused upwelling to stimulate ETM growth. This took

place principally in Tethys, because of its partial geographic isolation and circulatory restriction, leading to extreme ocean stratification.

5. The negative carbon isotope excursion associated with ETMs may be explained by interplay of negative-trending values from upwelled light carbon from the deep ocean (by whatever mechanism) and positive-trending values from microbial blooms (stimulated by phosphate-limited nutrient release).

6. Because ETMs seem to relate to concentration of deep ocean anoxia and carbonate in Tethys, their formation might be a predictable result of Early Triassic palaeogeography and climate, rather than being anachronistic. Thus the view expressed by some authors that earliest Triassic facies represent a "return to the past" does not fully acknowledge the combination of conditions in the run-up to the PTB events.

References

Alvarez W, O'Connor D (2002) Permian-Triassic boundary in the southwestern

United States: hiatus or continuity? In: Koerberl C, MacLeod KG (eds)

Catastrophic events and mass extinctions: impacts and beyond. Geol Soc

America Spec Pap 356: 385-393

Armella C (1994) Thrombolitic-stromatolitic cycles of the Cambro-Ordovician

boundary sequence, Precordillera Oriental Basin, western Argentina. In:

Bertrand-Sarfati J, Monty C (eds) Phanerozoic Stromatolites II. Kluwer

Academic Publishers, Dordrecht, pp 421-442

Baud A, Richoz S, Marcoux J (2005) Calcimicrobial cap rocks from the basal

Triassic units: western Taurus occurrences (SW Turkey). Comptes Rendus

Paleovol 4: 569-582.

Baud A, Richoz S, Pruss S (2006) The Lower Triassic anachronistic carbonate

facies in time and space. Global Planet Change 55: 81-89

Beauchamp B, Baud A (2002) Growth and demise of Permian biogenic chert

along northwest Pangaea: evidence for end-Permian collapse of thermohaline

circulation. Palaeogeogr Palaeoclimatol Palaeoecol 184: 37-63.

Berner RA (2005) The carbon and sulphur cycles and atmospheric oxygen from

middle Permian to middle Triassic. Geochim Cosmochim Acta 69: 3211-3217

Berner RA, Ward PD (2006) Positive reinforcement, H_2S, and the Permo-Triassic

extinction: comment. Geological Society of America Doi101130:G22641.1

Bissell HJ (1973) Permian-Triassic boundary in the eastern Great Basin area. In: Logan A, Hills LV (eds) Permian and Triassic systems and their mutual boundary. Can Soc Pet Geol Mem 2: 318-344

Bottrell SH, Newton RJ (2006) Reconstruction of changes in the global sulphur cycling from marine sulphate isotopes. Earth Sci Rev 75: 59-83

Brookfield ME, Twitchett RJ, Goodings C (2003) Palaeoenvironments of the Permian-Triassic transition sections in Kashmir, India. Palaeogeogr Palaeoclimatol Palaeoecol 198: 353-371

Calner M (2005) A Late Silurian extinction event and anachronistic period. Geology 33: 305-308

Chen D, Tucker ME, Shen Y, Yans J, Preat A (2002) Carbon isotope excursions and sea-level change: implications for the Frasnian-Famennian biotic crisis. J Geol Soc London 159: 623-626

Crasquin-Soleau S, Galfetti T, Bucher H, Brayard A (2006) Delayed marine faunal turnover after the end-Permian mass extinction: Early Triassic ostracods from northwestern Guangxi Province, south China. Riv It Paleontol Stratigr 112: 55-75

Crasquin-Soleau S, Kershaw S (2005) Ostracod fauna from the Permian-Triassic Boundary Interval of South China (Huaying Mountains, eastern Sichuan Province): palaeoenvironmental significance. Palaeogeogr Palaeoclimatol Palaeoecol 217: 131-141

Dill RF, Shinn EA, Jones AT, Kelly K, Steinen RP (1986) Giant subtidal stromatolites forming in normal salinity waters. Nature 324: 55-58.

Dravis JJ (1983) Hardened subtidal stromatolites, Bahamas. Science 219: 385-386

Erwin D H (2006) Extinction. Princeton University Press, 296pp

Escher A, Watt S W (1976) Geology of Greenland. The Geological Survey of Greenland. Copenhagen, 603pp

Ezaki Y, Liu J, Adachi N (2003) Earliest Triassic microbialite micro- to megastructures in the Huaying area of Sichuan Province, south China: implications for the nature of oceanic conditions after the end-Permian extinction. Palaios 18: 388-402

Fang Z (2006) Major bio-events in Permian-Triassic reef ecosystems of south China and their bearing on extinction-survival-recovery problems. In: Rong J, Fang Z (eds) Mass extinction and recovery; evidences from the Palaeozoic and Triassic of South China, Vol II.1063-1065. University of Science and Technology of China Press.

Flügel E (2002) Triassic Reef Patterns. In: Kiessling W, Flügel E, Golonka J (eds) Phanerozoic reef patterns. SEPM Spec Publ 72: 391-463

Foster CB, Afonin SA (2005) Abnormal pollen grains: an outcome of deteriorating atmospheric conditions around the Permian-Triassic boundary. J Geol Soc 162: 653-659

Fraiser ML, Twitchett RJ, Bottjer DJ (2005) Unique microgastropod facies in the Early Triassic: indicator of long-term biotic stress and the pattern of biotic recovery after the end-Permian mass extinction. Comptes Rendus Palevol 4: 543-552

Garzanti E, Nicora A, Rettori R (1998) Permo-Triassic boundary and lower to middle Triassic in south Tibet. J Asian Earth Sci 16: 143-157

Goldhammer RK, Lehmann PJ, Dunn PA (1993) The origin of high-frequency platform carbonate cycles and third-order sequences (Lower Ordovician El Paso Gp, West Texas): constraints from outcrop data and stratigraphic modelling. J Sediment Petrol 63: 318-359

Golonka J (2002) Plate-tectonic maps of the Phanerozoic. In: Kiessling W, Flügel E, Golonka J (eds) Phanerozoic Reef Patterns. SEPM Spec Publ 72: 21–76.

Grice K, Cao C-Q, Love GD, Böttcher ME, Twitchett RJ, Grosjean E, Summons RE, Turgeon SC, Dunning W, Jin Y-G (2005a) Photic zone euxinia during the Permian-Triassic superanoxic event. Science 307: 706-709

Grice K, Twitchett RJ, Alexander R, Foster CB, Looy C (2005b) A potential biomarker for the Permian-Triassic ecological crisis. Earth Planet Sci Lett 236: 315-321

Grotzinger JP, Knoll AH (1995) Anomalous carbonate precipitates: is the Precambrian the key to the Permian? Palaios 10: 578-596

Haas J, Demény A, Hips K, Vennemann TW (2006) Carbon isotope excursions and microfacies changes in marine Permian-Triassic boundary sections in Hungary. Palaeogeogr Palaeoclimatol Palaeoecol 237: 160-181

Heydari E, Hassandzadeh J, Wade WJ (2000) Geochemistry of central Tethyan Upper Permian and Lower Triassic strata, Abadeh region, Iran. Sediment Geol 137: 85-99

Hips K, Haas J (2006) Calcimicrobial stromatolites at the Permian-Triassic

boundary in a western Tethyan section, Bükk, Hungary. Sediment Geol 185: 239-253

Hotinski RM, Bice KL, Kump LR, Naijir RG, Arthur MA (2001) Ocean stagnation and end-Permian anoxia. Geology, 29, 7-10

Isozaki Y (1997) Permo-Triassic superanoxia and stratified superocean: records from the lost deep sea. Science, 276: 235-238

Kaiho K, Chen Z-Q, Kawahata H, Kajiwara Y, Sato H (2006) Close-up of the end-Permian mass extinction horizon recorded in the Meishan section, South China: sedimentary, elemental, and biotic characterization and a negative shift of sulphate sulphur isotope ratio. Palaeogeogr Palaeoclimatol Palaeoecol 239: 396-405

Kakuwa Y, Matsumoto R (2006) Cerium negative anomaly just before the Permian and Triassic boundary event – the upward expansion of anoxia in the water column. Palaeogeogr Palaeoclimatol Palaeoecol 229: 335-344

Kempe S (1990) Alkalinity: the link between anaerobic basins and shallow water carbonates? Naturwissenschaften 77: 426-427

Kennard JM (1994) Thrombolites and stromatolites within shale-carbonate cycles, Middle-Late Cambrian Shannon Formation, Amadeus Basin, central Australia. In: Bertrand-Sarfati J, Monty C (eds) Phanerozoic Stromatolites II. Kluwer Academic Publishers, Dordrecht, pp 443 – 741

Kershaw S (2004) Comment - Earliest Triassic microbialite micro- to megastructures in the Huaying area of Sichuan Province, south China:

implications for the nature of oceanic conditions after the end-Permian extinction (Ezaki et al. 2003). Palaios 19: 418-420

Kershaw S, Zhang T, Lan G (1999) A ?microbialite crust at the Permian-Triassic boundary in south China, and its palaeoenvironmental significance. Palaeogeogr Palaeoclimatol Palaeoecol 146: 1-18

Kershaw S, Guo L, Swift A, Fan J (2002) ?Microbialites in the Permian-Triassic boundary interval in central China: structure, age and distribution. Facies 47: 83-90

Kidder DL, Worsley TR (2004) Causes and consequences of extreme Permo-Triassic warming to globally equable climate and relation to the Permo-Triassic extinction and recovery. Palaeogeogr Palaeoclimatol Palaeoecol 203: 207-237

Kiehl JT, Shields CA (2005) Climate simulation of the latest Permian: implications for mass extinction. Geology 33: 757-760

Krull ES, Lehrmann DJ, Druke D, Kessel B, Yu Y, Li R (2004) Stable carbon isotope stratigraphy across the Permian-Triassic boundary in shallow marine carbonate platforms, Nanpanjiang Basin, South China. Palaeogeogr Palaeoclimatol Palaeoecol 204: 297-315

Krystyn L, Richoz S, Baud A, Twitchett R (2003) A unique Permian-Triassic boundary section from the Neotethyan Hawasina Basin, Central Oman Mountains. Palaeogeogr Palaeoclimatol Palaeoecol 191: 329-344

Kump LR (2005) Massive release of hydrogen sulphide to the surface ocean and atmosphere during intervals of ocean anoxia. Geology 33: 397-400

Kump LR, Pavlov A, Arthur MA (2006). Positive reinforcement, H_2S, and the
Permo-Triassic extinction: reply. Geological Society of America
Doi10.1130/G22836.1

Lehrmann DJ (1999) Early Triassic calcimicrobial mounds and biostromes of the
Nanpanjiang Basin, South China. Geology 27: 359-362

Lehrmann DJ, Wan Y, Wei J, Yu Y, Xiao J (2001) Lower Triassic peritidal cyclic
limestone: an example of anachronistic carbonate facies from the Great Bank
of Guizhou, Nanpanjiang Basin, Guizhou Province, South China.
Palaeogeogr Palaeoclimatol Palaeoecol 173: 103-123

Lehrmann DL, Payne JL, Felix SV, Dillett PM, Wang H, Yu Y, Wei J (2003)
Permian-Triassic boundary sections from shallow-marine carbonate platforms
of the Nanpanjiang Basin, south China: Implications for oceanic conditions
associated with the end-Permian extinction and its aftermath: Palaios 18:
138-152

Liu J, Ezaki Y, Yang S (2006) High-resolution environmental reconstruction of the
aftermath of the end-Permian mass extinction: evidence from microbialite
successions in South China. In: Yang Q, Wang Y, Weldon E (eds) Ancient
life and modern approaches. Abstracts of the Second International
Palaeontological Congress, Beijing, 17-21 June 2006, p 208-209

Mu X, Guo L, Kershaw S, Qi Y (2001) The microbialite crust at Permian-Triassic
boundary interval in E. Sichuan, China. In: Bucur I, Tantau I (eds) 4th
Regional Symposium of I.F.A.A. , August 29 – September 5, 2001, Cluj-
Napoca, Romania, Abstracts, p 38-39

Payne J, Lehrmann DJ, Wei J, Orchard MJ, Schrag DP, Knoll AH (2004) Large perturbations of the carbon cycle during recovery from the end-Permian extinction. Science 305: 506-509

Perch-Nielsen K, Bromley RG, Birkenmajer K, Aellen M (1972) Field observations in Palaeozoic and Mesozoic sediments of Scoresby Land and northern Jameson Land. Rapp Gronl Geol Unders 48: 39-59

Pruss SB, Bottjer DJ, Corsetti FA, Baud A (2006) A global marine sedimentary response to the end-Permian mass extinction: examples from southern Turkey and the western United States. Earth Sci Rev 78: 193-206

Riding R (2000) Microbial carbonates: the geological record of calcified bacterial-algal mats and biofilms. Sedimentology 47 (Suppl 1): 179-214

Riding R (2005) Phanerozoic reefal microbial carbonate abundance: comparisons with metazoan diversity, mass extinction events, and seawater saturation state. Rev Esp de Micropaleontol 37: 23-39

Riding R, Liang L (2005) Geobiology of microbial carbonates: metazoan and seawater saturation state influences on secular trends during the Phanerozoic. Palaeogeogr Palaeoclimatol Palaeoecol 219: 101-115

Ryskin G (2003) Methane-driven oceanic eruptions and mass extinctions. Geology 31: 741-744

Saltzman MR (2005) Phosphorus, nitrogen, and the redox evolution of the Palaeozoic oceans. Geology 33: 573-576

Sandler A, Eshet Y, Schilman B (2006) Evidence for a fungal event, methane hydrate release and soil erosion at the Permian-Triassic boundary in southern Israel. Palaeogeogr Palaeoclimatol Palaeoecol 242: 68-89

Sano H, Nakashima K (1997) Lowermost Triassic (Griesbachian) microbial bindstone-cementstone facies, southwest Japan. Facies 36: 1-24

Schubert JK, Bottjer DJ (1992) Early Triassic stromatolites as post-mass extinction disaster forms. Geology 20: 883-886

Sephton MA, Looy CV, Brinkhuis H, Wignall PB, de Leeuw JW, Visscher H (2005) Catastrophic soil erosion during the end-Permian biotic crisis. Geology 33: 941-944

Sepkoski JJ Jr, Bambach RK, Droser ML (1991) Secular changes in Phanerozoic event bedding and the biological overprint. In: Einsele G, Ricken W, Seilacher A (eds) Cycles and events in stratigraphy. Berlin, Springer, p. 298-312

Sheehan P, Harris M (2004) Microbialite resurgence after the late Ordovician extinction. Nature 430: 75-78

Sheldon N (2006) Abrupt chemical weathering increase across the Permian-Triassic boundary. Palaeogeogr Palaeoclimatol Palaeoecol 231: 315-321

Tong J, Yin H (2002) The Lower Triassic of South China. J Asian Earth Sci 20: 803-815

Twitchett RJ (2004) Trace fossils in the aftermath of mass extinction events. In: McIlroy D (ed) The application of ichnology to palaeoenvironmental stratigraphic analysis. Geol Soc Lond Spec Publ 238: 397-418

Twitchett RJ (2006) The palaeoclimatology, palaeoecology and palaeoenvironmental analysis of mass extinction events. Palaeogeogr Palaeoclimatol Palaeoecol 232: 190-213

Twitchett RJ, Krystyn L, Baud A, Wheeley JR, Richoz S (2004) Rapid marine recovery after the end-Permian mass-extinction event in the absence of marine biota. Geology 32: 805-808

Valentine JW, Moores EM (1973) Provinciality and diversity across the Permian-Triassic boundary. In: Logan A, Hills LV (eds) Permian and Triassic systems and their mutual boundary. Can Soc Pet Geol Mem 2: 759-766

Wang S, Qiang Z, Wen Y, Tao Y (1994) Petrology and origin of the calcareous crusts capping the Permian reefs in Huaying Mountains, Sichuan, China. J Mineral Petrol 14: 59-68 (in Chinese)

Wang W, Matsumoto R, Kakuwa Y, Mahmudy Gharaie MH, Li Y, Kano A, Matsuda N, Jansa L, Ueno K, Milroy P, Rahmati Ilkhchi M (2005) Chemostratigraphy of Carbon and Strontium Isotope on Permo-Triassic Boundary in Zagros Moutains, Aligoudarz, Iran. Permophiles 45: 31-36

Wang Y, Jin Y (2000) Permian palaeogeographic evolution of the Jiangnan Basin, South China. Palaeogeogr Palaeoclimatol Palaeoecol 160: 35-44

Weidlich O, Kiessling W, Flügel E (2003) Permian-Triassic boundary interval as a model for forcing marine ecosystem collapse by long-term atmospheric oxygen drop. Geology 31: 961-964

Whalen MT, Day J, Eberli GP, Homewood PW (2002) Microbial carbonates as indicators of environmental change and biotic crises in carbonate systems:

examples from the Late Devonian, Alberta Basin, Canada. Palaeogeogr Palaeoclimatol Palaeoecol 181: 127-151

Wignall PB, Hallam A (1992) Anoxia as a cause of the Permian/Triassic mass extinction: facies evidence from northern Italy and the western United States. Palaeogeogr Palaeoclimatol Palaeoecol 93: 21-46

Wignall PB, Hallam A (1993) Griesbachian (Earliest Triassic) palaeoenvironmental changes in the Salt Range, Pakistan, and southeast China and their bearing on the Permo-Triassic mass extinction. Palaeogeogr Palaeoclimatol Palaeoecol 102: 215-237

Wignall PB, Twitchett RJ (2002) Extent, duration and nature of the Permian-Triassic superanoxic event. In: Koerberl C, MacLeod KG (eds) Catastrophic events and mass extinctions: impacts and beyond. Geol Soc America Spec Pap 356: 395-413

Winguth AME, Maier-Reimer E (2005) Causes of the marine productivity and oxygen changes associated with the Permian-Triassic boundary: a reevaluation with ocean general circulation models. Mar Geol 217: 283-304

Woods AD, Bottjer DJ, Mutti M, Morrison J (1999) Lower Triassic large sea-floor carbonate cements: their origin and a mechanism for the prolonged biotic recovery from the end-Permian mass extinction. Geology 27: 645-648

Yang H, Zhang S, Jiang H, Wang Y (2006) Age and general characteristics of calcimicrobialite near the Permian-Triassic boundary in Chongyang, Hubei Province. Earth Sci J China 31: 165-170

FIGURE CAPTIONS

Fig. 1 A Earliest Triassic global palaeogeography (base map from Golonka 2002), with locations of microbialite deposits. Ocean circulation and sites of upwelling (u) and sinking (s) (Kidder and Worsley 2004) are shown. 1 & 2: northern and southern South China respectively; 3: Iran; 4: Turkey; 5: Japan; 6: Hungary; 7: Utah & Nevada; 8: Greenland; 9: Italy; 10: Tibet, Kashmir & Pakistan; 11: Oman; 12: Madagascar. Note that 1-4 form the Cimmerian continents and are located in low latitudes (according to this plate reconstruction) where upwelling is most likely. **B** Enlargement of South China Block showing relative locations of sites 1 & 2 in **A**; the two sites are c.600 km apart

Fig. 2 A Schematic reconstruction of ETM from Baizhuyuan, northern SCB (see Kershaw et al. 1999 for locality details). The vertical scale is a measured section (updated from Kershaw et al. 1999), and details of the reconstruction were formed from lateral variations in the site. Details of the microbialite are simplified for clarity. Note: sharp base of microbialite; interlayered thrombolite and digitate; interlayered shelly micrite; the microbialite top is stylolitised, but its undulose upper margin is clear. **B** Polished block of outlined area in **A**, showing the thrombolitic lower fabric, and digitate upper fabric, as well as undulose boundary, and separation of the two microbial phases by micritic sediment

Fig. 3 A Enlargement of area of boundary between thrombolitic and digitate fabrics from Fig. 2, for the Baizhuyuan locality. Note the sediment break between the two microbial portions. **B** Photomicrograph of the contact area in **A**; width of photo 2 mm. **C** Photomicrograph of the thrombolite in **A**; width of photo 1.8 mm.

Fig. 4 Field photographs of Early Triassic microbialites at Dongwan, Sichuan (see Ezaki et al. 2003 for locality details). **A** General view showing layered microbialite. Lower rocks are the underlying Permian Changhsing Formation limestones. **B** Detail of base of microbialite, showing digitate dendrolitic fabric, stylolitised contact, and underlying Permian limestones. **C** Central portion of microbialite sequence, showing digitate microbialite overlain by shell-rich wackestone, which is an interlayer of sediment interrupting the microbialite. **D** Detail of central part of microbialite showing two digitate dendrolitic domes separated by micrite. **E** Detail of a dendrolitic (not digitate dendrolitic) fabric, which forms a minor part of the microbialite. **F** Detail of upper part of microbialite, which consists of isolated domes of digitate fabric, that have been partly eroded. These are the domes shown in detail in Fig. 5B and C, and reconstructed in three dimensions in Fig. 7

Fig. 5 Polished blocks of microbialite from Dongwan. **A** Detail of top of one layer of digitate dendrolite, from the central part of the microbialite 200 m from the measured site in Fig. 7. Note eroded upper surface, overlain by shell-rich micrite.

Stylolites affect this sample. Scale bar 1 cm. **B** and **C** Details of upper part of microbialite showing isolated small domes of digitate dendrolite, with micrite fill showing a least two episodes of erosion (**B**), and eroded margins of domes; these samples are from the same horizon illustrated in Fig. 4F

Fig. 6 Photomicrographs of microbialites at Dongwan. **A** Central portion of sequence, showing poorly-developed digitate fabric. Photo width 2.5 mm. **B** Top of microbialite from a small dome in Fig. 5, showing eroded tip of a digitate branch that has a lobate margin on left hand side. Note gastropod packstone overlying eroded microbia, and the eroded top surface of the dark-coloured micrite. Photo width 0.5 mm. **C** Enlargement of **B**, showing small crystal fan on eroded tip, and poorly-preserved microbial fabric. Photo width 2.5 mm. **D** Enlargement of **B**, showing lobate margin. Photo width 0.5 mm. In **A**, the micrite has no peloids, contrasting **B-D** where the sediment is composed almost entirely of peloids. See text for discussion

Fig. 7 Schematic reconstruction of Dongwan microbialite. The vertical scale is a measured section and details of the reconstruction were formed from lateral variations in the site. Details of the microbialite are simplified for clarity. Note: sharp base (stylolitised, but not shown here); tabular lower portion, domal upper portion, shell-rich sediment interlayer, and isolated domes at top. Micritic sediment occupies space between microbialite digitate fabric; micrite in the

interlayer and in the top few mm of microbialite is peloid-rich; otherwise the

micrite contains little peloidal fabric

Fig. 8 A Field view of base of microbialite at Rungbuo site, GBG, Guizhou

Province (see Lehrmann 1999). Note eroded Permian limestones and

encrustation of the microbialite framestone. **B** and **C** Polished vertical sections of

base of microbialite and underlying Permian grainstones. Note: variation in frame

of microbialite, with some sparite filling cavities; in **B**, there are two-phases of

erosion of the Permian limestone. **D** Transverse section of microbialite, showing

irregular nature of framestone

Fig. 9 Vertical thin section of stromatolite from Aliguoardarz, Iran. Scale bar 1 cm

Fig. 10 Reconstruction model of controls on formation of Earliest Triassic

Microbialites, emphasising aspects of topography, anoxia and bicarbonate input.

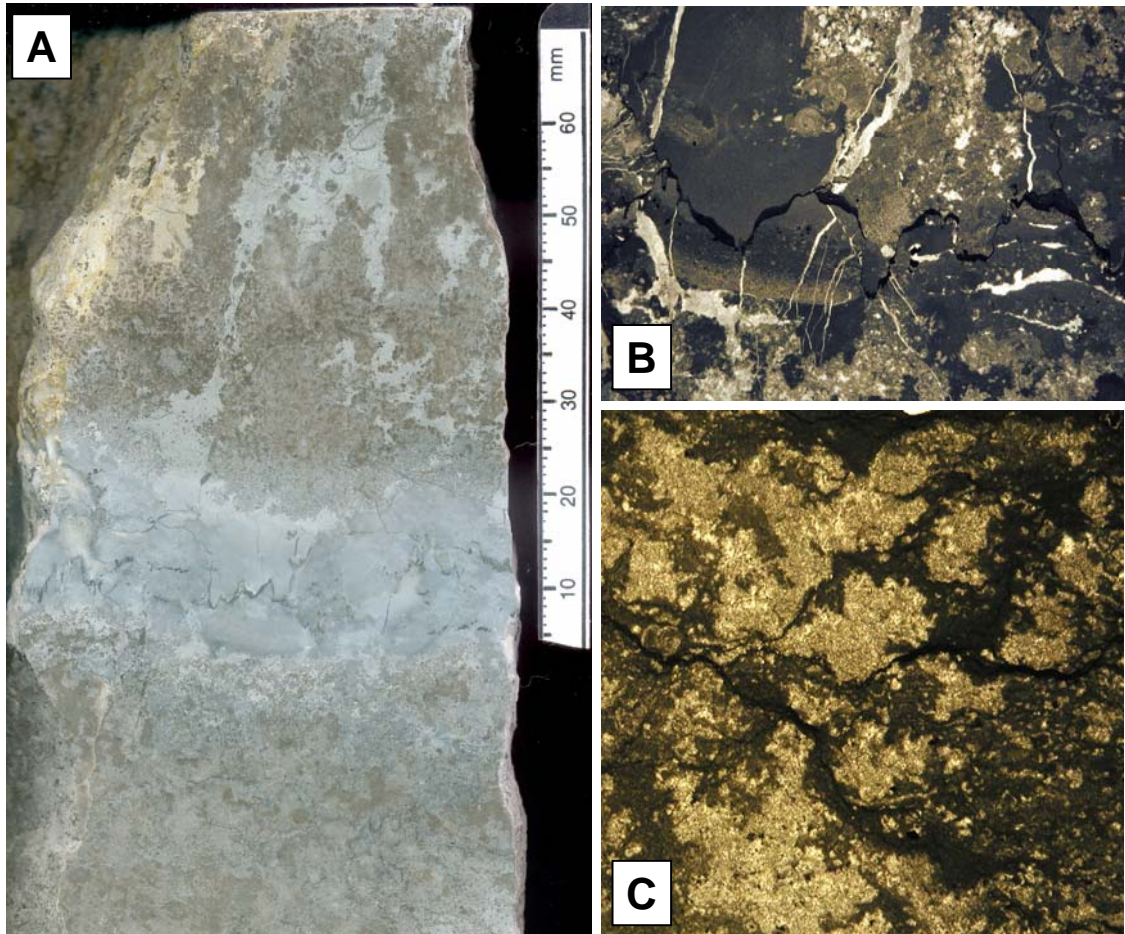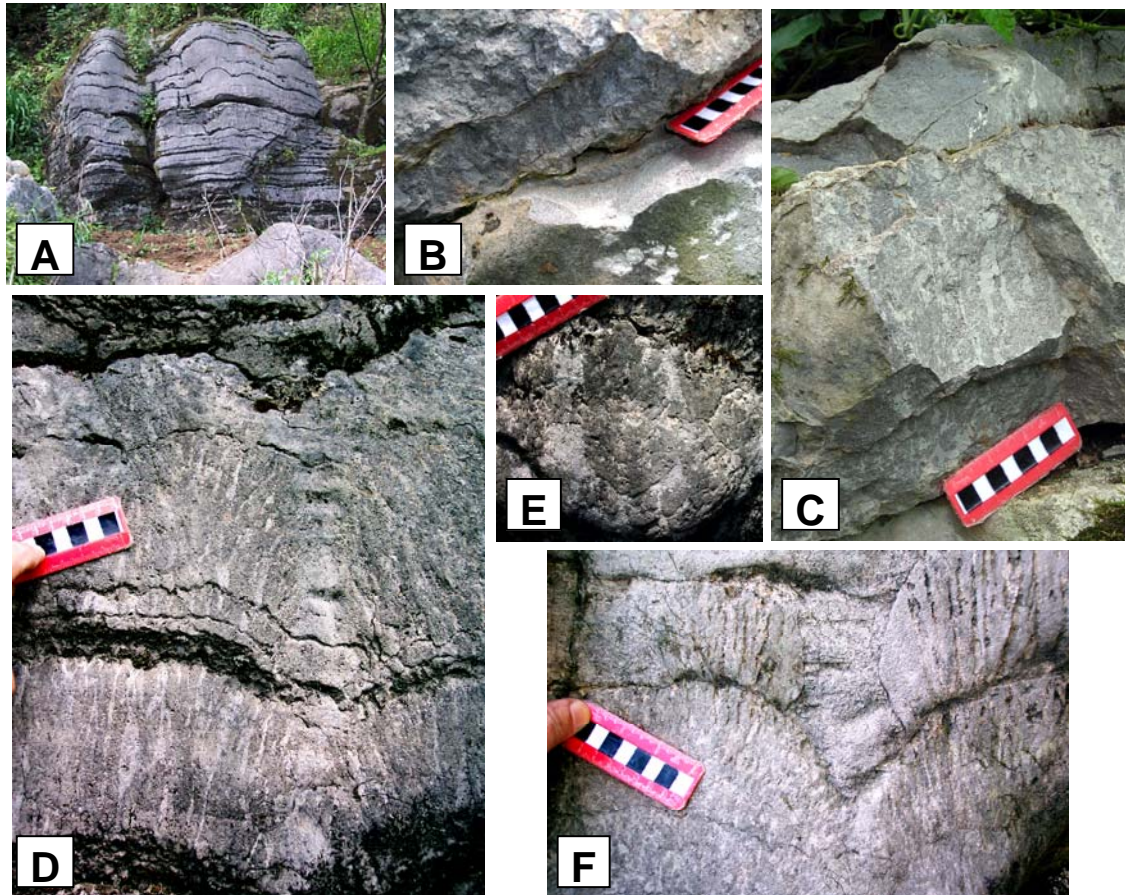This model is updated from Kershaw et al. (1999); see text for discussion

Figure 1
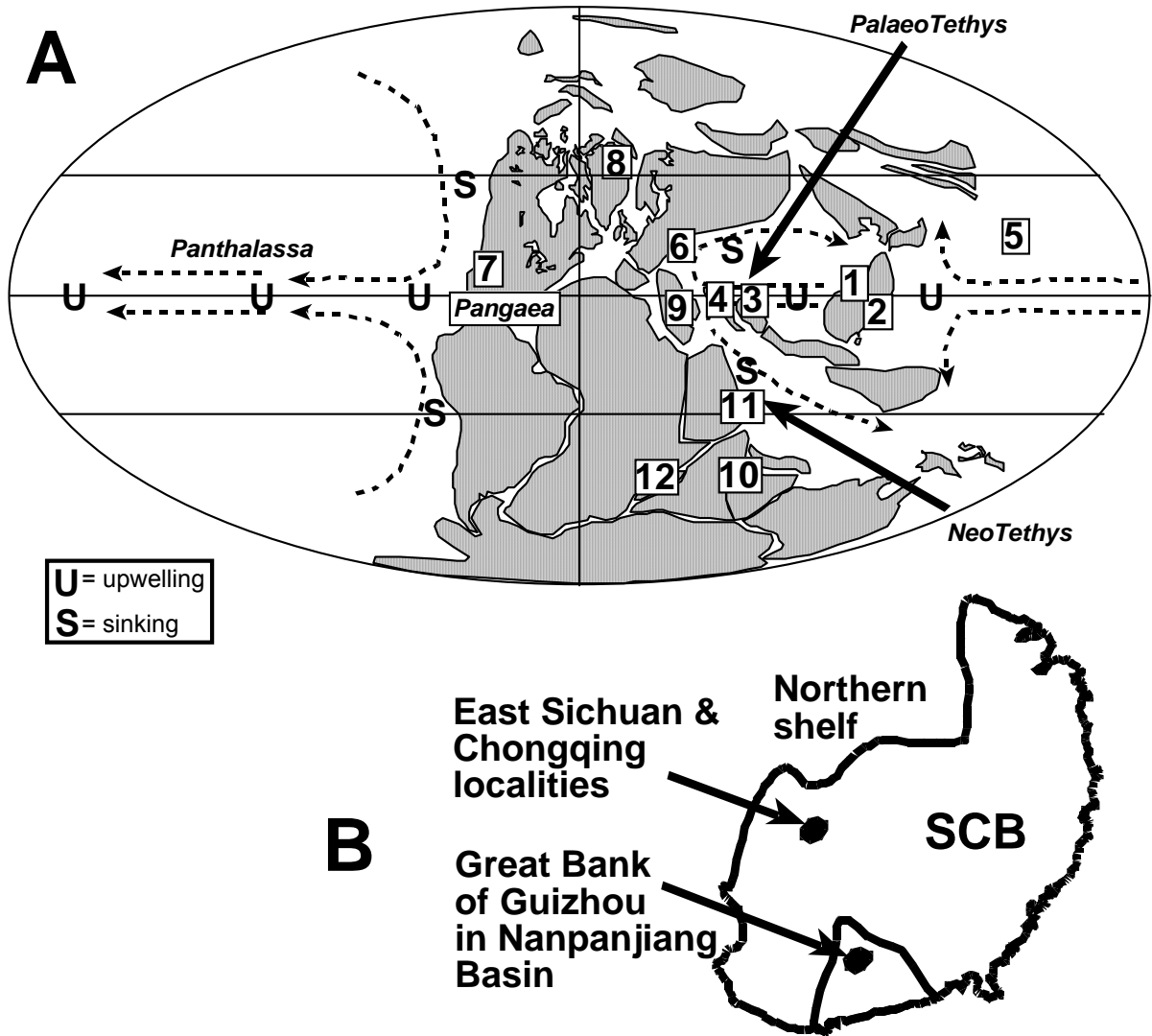
Figure 2
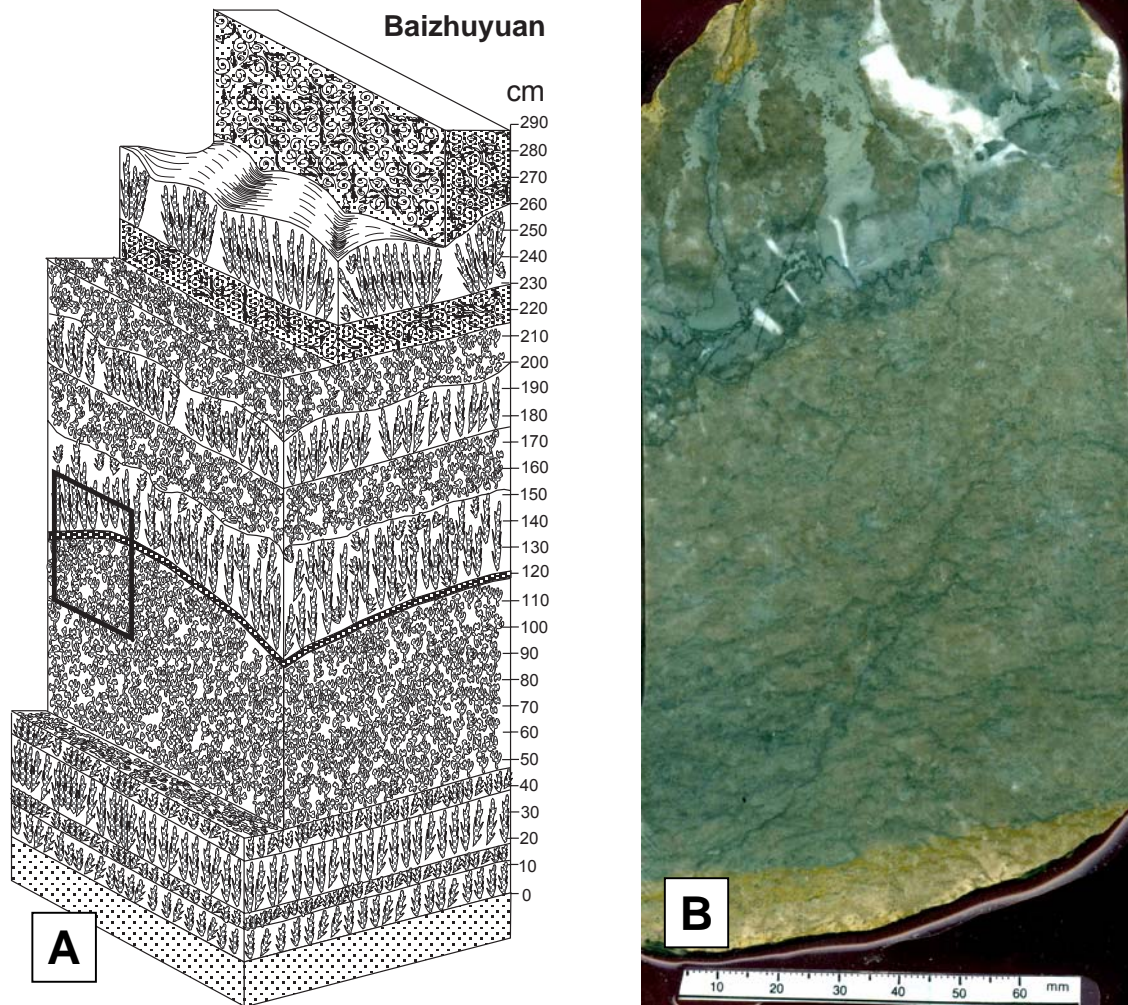
Figure 3

Figure 4

Figure 5

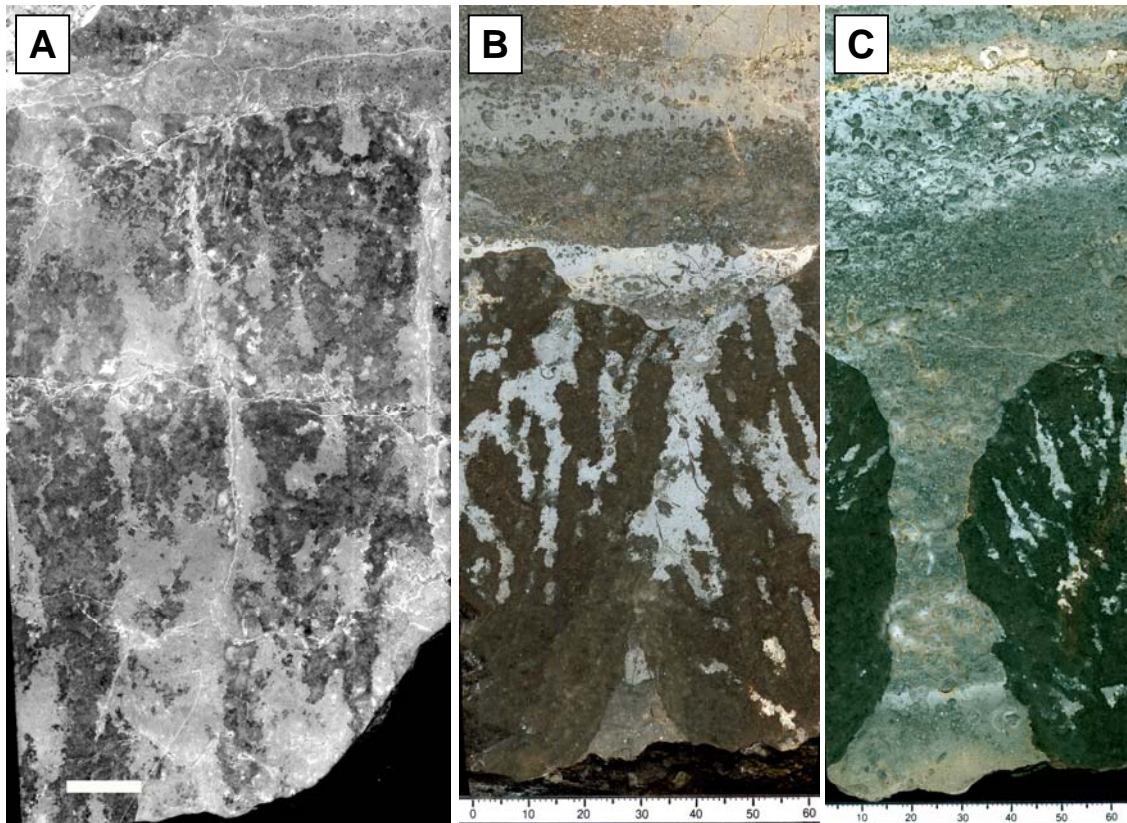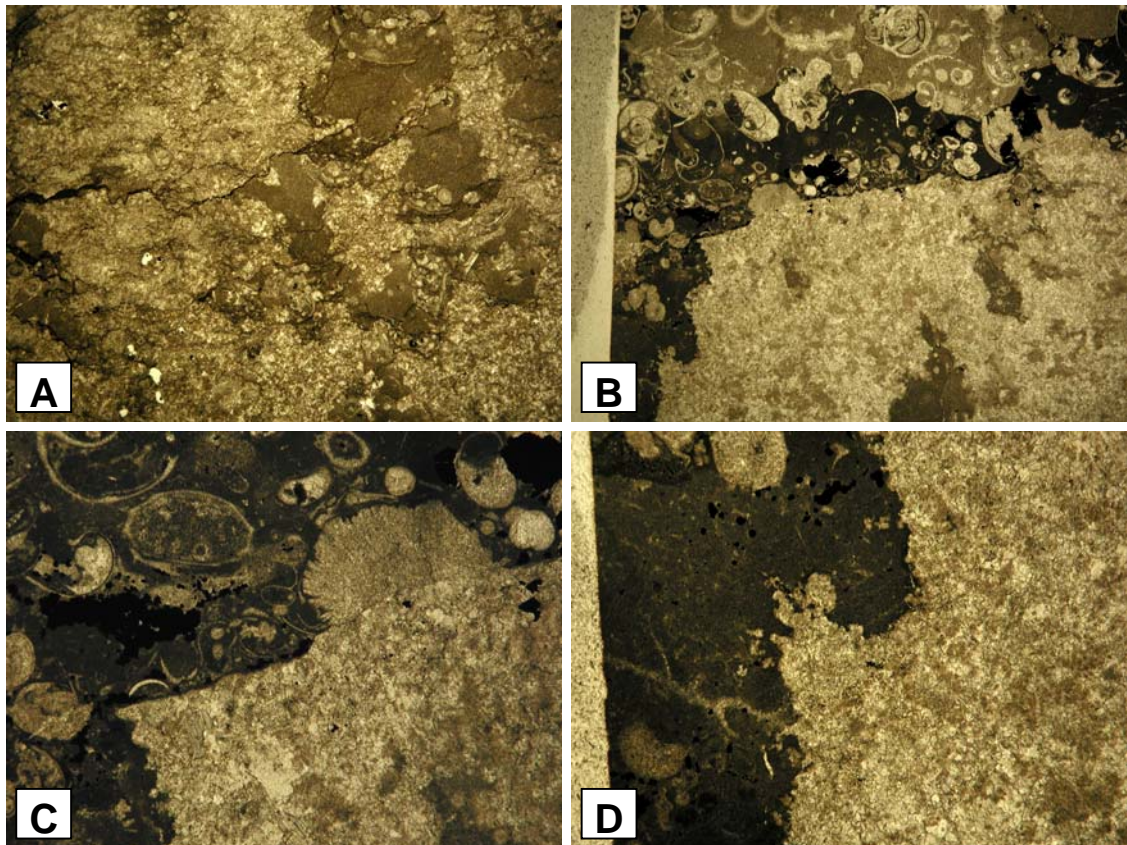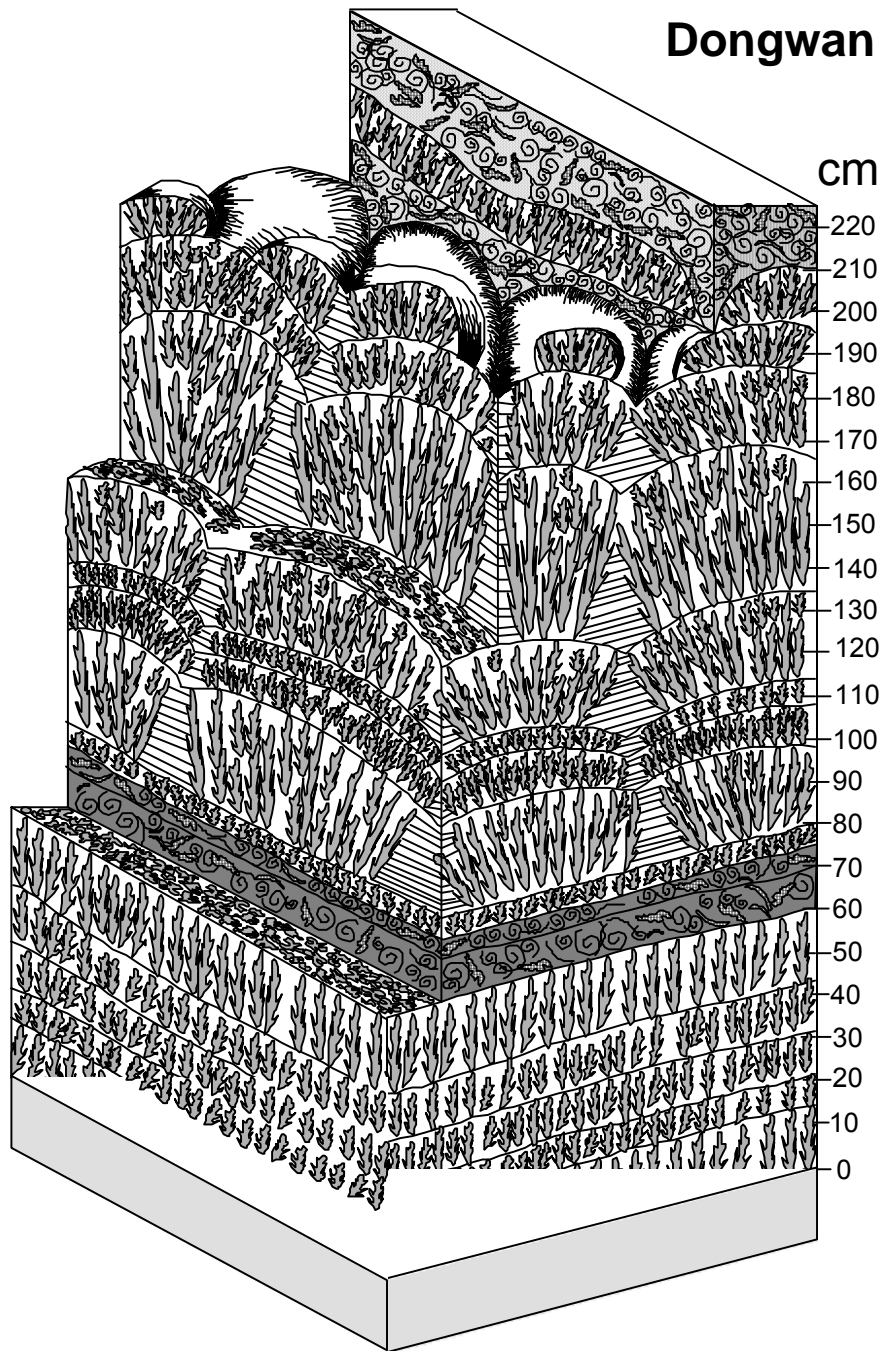Figure 6

Figure 7

Figure 8

Figure 9

Figure 10

**Redox boundary
in the water column;
microbialite grew
above it**

**Upwelled oxygen-poor,
bicarbonate-rich water
stimulated microbialite
growth**

**Microbialite grew
in shallow waters,
including topographic highs,
possibly as a disaster biota;
regional variations in microbialite
architecture and composition**

**Shallow water Late Permian
fossiliferous limestones (reefs
and overlying crinoidal grainstones)**